

Quantum entanglement dynamics of the three-qubit W_ζ quantum state coupled to spin chain with ternary interaction

S. M. Moosavi Khansari¹

Department of Physics, Faculty of Basic Sciences, Ayatollah Boroujerdi University, Boroujerd, IRAN

F. Kazemi Hasanvand

Department of Physics, Faculty of Basic Sciences, Ayatollah Boroujerdi University, Boroujerd, IRAN

In this study, we explore the dynamics of quantum entanglement using the negativity criterion for the W_ζ quantum state. We investigate changes in negativity in terms of anisotropy parameters, γ , the strength of the external magnetic field applied to the spin chain, η , the triple interaction strength, α . We examine how these parameters affect the entanglement properties of the system and discuss the implications for quantum information processing and quantum communication protocols. By analyzing the negativity of the W_ζ state under different conditions, we gain insights into the behavior of entanglement in complex quantum systems. Our results shed light on the intricate interplay between various factors that influence quantum entanglement and provide a foundation for further investigations in this field of research.

Keywords: Anisotropy, Negativity, Quantum entanglement, W_ζ quantum state

1 Introduction

Quantum entanglement, as a key aspect of quantum theory, has garnered significant interest in recent years. Its nonlocal correlations between quantum systems are crucial in quantum information processing. Quantum entanglement is the bases of several tasks in quantum information and computation [1-8]. However, real-world non-local entanglement is often sensitive to decoherence, which refers to the loss of quantum coherence as a system interacts with its environment. This intricate quantum phenomenon poses challenges, leading to diverse studies using various models [9-16]. Presently, there is a growing focus on investigating decoherence within systems featuring a spin environment exhibiting a quantum phase transition at zero temperature induced by pure quantum fluctuations [17-24]. In this context, understanding entanglement as a geometric phase [25] and analyzing fidelity [26] are fundamental for studying quantum phase transitions. In prior research, attention was primarily given to the nearest spin-spin interactions in spin chains. However, in practical applications, it becomes essential to delve into quantum spin models that accurately account for not only nearest neighbour interactions but also consider nearest neighbour spin exchange models or multiple spin exchange models [27, 28, 29,

¹ Email of the corresponding author: m.moosavikhansari@abru.ac.ir
(m.moosavikhansari@gmail.com)

30, 31]. Research in this area has thus expanded to encompass more sophisticated quantum spin models that can better capture the intricacies of real-world systems. By considering not only nearest neighbor interactions but also incorporating nearest neighbor spin exchange models or even multiple spin exchange models, researchers hope to gain deeper insights into the behavior of these quantum systems. Studies involving these more complex models, such as those proposed by Tsvelik et al. [23], Frahm et al. [24], Zvyagin [25], and others, are shedding light on the effects of various interactions on quantum entanglement and decoherence in spin environments. By exploring these richer models, scientists aim to improve our understanding of quantum phase transitions and pave the way for more advanced applications of quantum information processing technologies [32-36].

This study investigates entanglement dynamics in a qubit system embedded in a spin chain environment. The organization of the rest of this paper is as follows: In Sec. 2, we introduces the model and derives the time-dependent density operator. In Section 3, the W_ξ state is introduced, followed by the derivation of its time-dependent density matrix and the calculation of measures from Section 2. Finally, section 4 is devoted to discussion and conclusions.

2 Hamiltonian and the time dependent density matrix

In this article, we express the Hamiltonian of the entire composite system with the following relation

$$H = H_0 + H_I \quad (1)$$

where

$$H_0 = -\sum_{k=-M}^M \alpha (\sigma_{k-1}^x \sigma_k^z \sigma_{k+1}^y - \sigma_{k-1}^y \sigma_k^z \sigma_{k+1}^x) - \sum_{k=-M}^M \left(\frac{1}{2} (\gamma + 1) \sigma_k^x \sigma_{k+1}^x + \frac{1}{2} (1 - \gamma) \sigma_k^y \sigma_{k+1}^y + \eta \sigma_k^z \right) \quad (2)$$

expresses the spin chain Hamiltonian of Inthe environment with the $XZY - YZX$ triplet interaction and

$$H_I = \sum_{k=-M}^M (-g_A \sigma_A^z - g_B \sigma_B^z - g_C \sigma_C^z) \sigma_k^z \quad (3)$$

is the Hamiltonian of the interaction between the three-qubit system and the spin chain of the environment. In these relations, $\sigma_A^z, \sigma_B^z, \sigma_C^z$ and σ_k^x, σ_k^y and σ_k^z are Pauli operators that describe the three qubits and the spin chain of the environment. The parameter $M = (N - 1)/2$ is defined for odd N , where N is the number of particles in the spin chain. The parameter γ determines the anisotropy in the in-plane interaction, while η expresses the strength of the externally applied transverse field to the environment. The parameters g_A, g_B , and g_C represent the coupling strength between the three-qubit system and the spin chain of the environment. The parameter α describes the strength of the $XZY - YZX$ triplet interaction. This establishes the following quantum commutator

$$[g_A \sigma_A^z + g_B \sigma_B^z + g_C \sigma_C^z, \sigma_k^{x,y,z}] = 0 \quad (4)$$

Therefore, the total Hamiltonian can be expressed as follows

$$H = \sum_{\mu=1}^8 |\phi_\mu\rangle\langle\phi_\mu| \otimes H_E^{\lambda_\mu} \quad (5)$$

where $|\phi_\mu\rangle$ represents the μ th eigenstate of the operator $(g_A \sigma_A^z + g_B \sigma_B^z + g_C \sigma_C^z)$ and $|000\rangle, \dots, |111\rangle$ corresponding to the μ th eigenvalue of g_μ are taken into account. Additionally,

$\lambda_\mu = \eta + g_\mu$, and these values are defined by the following expressions

$$\lambda_1 = g_A + g_B + g_C + \eta, \quad \lambda_2 = g_A + g_B - g_C + \eta \quad (6)$$

$$\lambda_3 = g_A - g_B + g_C + \eta, \quad \lambda_4 = g_A - g_B - g_C + \eta \quad (7)$$

$$\lambda_5 = -g_A + g_B + g_C + \eta, \quad \lambda_6 = -g_A + g_B - g_C + \eta \quad (8)$$

$$\lambda_7 = -g_A - g_B + g_C + \eta, \quad \lambda_8 = -g_A - g_B - g_C + \eta \quad (9)$$

To determine the entanglement dynamics of the target three-qubit system, acquiring the time evolution operator $U(t) = \exp(-iHt)$ is essential. Given the initial state of the system, $\rho(0)$, we can derive the quantum state's time evolution using $\rho(t) = U(t)\rho(0)U(t)^\dagger$. Utilizing the Jordan-Wigner transformation, which converts the spin system into a quasi-Fermi system

$$\sigma_k^z = 1 - 2c_k^\dagger c_k, \quad \sigma_k^+ = [\prod_{m<k} (1 - 2c_m^\dagger c_m)]c_k, \quad \sigma_k^- = [\prod_{m<k} (1 - 2c_m^\dagger c_m)]c_k^\dagger \quad (10)$$

and the Fourier transform

$$d_\ell = \frac{1}{\sqrt{N}} \sum_k c_k \exp(-2\pi i k \ell / N) \quad (11)$$

and Bogolyubov transformation

$$b_{\ell, \lambda_\mu} = d_\ell \cos \frac{\theta_\ell^{\lambda_\mu}}{2} - i d_{-\ell}^\dagger \sin \frac{\theta_\ell^{\lambda_\mu}}{2} \quad (12)$$

where

$$\tan(\theta_\ell^{\lambda_\mu}) = \frac{\gamma \sin(\frac{2\pi\ell}{N})}{(\lambda_\mu - \cos(\frac{2\pi\ell}{N}))} \quad (13)$$

the $H_E^{\lambda_\mu}$ Hamiltonian can be accurately diagonalized as [26]

$$H_E^{\lambda_\mu} = \sum_{k=-M}^M \xi_k^{\lambda_\mu} \left(b_{k, \lambda_\mu}^\dagger b_{k, \lambda_\mu} - \frac{1}{2} \right) \quad (14)$$

the energy spectrum can be expressed as

$$\xi_k^{\lambda_\mu} = 2\alpha \sin\left(\frac{4\pi k}{N}\right) + 2 \sqrt{\gamma^2 \sin^2\left(\frac{2\pi k}{N}\right) + \left(\lambda_\mu - \cos\left(\frac{2\pi k}{N}\right)\right)^2} \quad (15)$$

With these interpretations, we can explore the dynamic evolution of the three-qubit system. We assume that the three-qubit system and the spin chain of the environment initially have a density matrix in the form of the following tensor product

$$\rho(0) = \rho_{ABC}(0) \otimes \rho_E(0) \quad (16)$$

where $\rho_{ABC}(0)$ and $\rho_E(0)$ represent the initial density matrix of the three-qubit system and the density matrix of the spin chain of the environment, respectively. Now, we assume that the three-qubit system is initially in the state $\rho_{ABC}(0) = \sum_{\mu, \nu} |\phi_\mu\rangle\langle\phi_\nu|$, while the spin chain of the environment is initially in thermal equilibrium state as follows

$$\rho_E(0) = \frac{1}{Z} \exp(-\beta \sum_k \xi_k b_k^\dagger b_k) \quad (17)$$

where $\beta = \frac{1}{kT}$ and we can express

$$\xi_k = 2\alpha \sin\left(\frac{4\pi k}{N}\right) + 2\sqrt{\gamma^2 \sin^2\left(\frac{2\pi k}{N}\right) + \left(\eta - \cos\left(\frac{2\pi k}{N}\right)\right)^2} \quad (18)$$

and

$$Z = \text{Tr}[\exp(-\beta \sum_k \xi_k b_k^\dagger b_k)] \quad (19)$$

where Z represents the partition function of the spin chain environment. Upon formulating the time evolution of the entire system and tracing the environment spin chain variable, the reduced density matrix $\rho_{ABC}(t) = \text{Tr}_E[U(t)\rho(0)U(t)^\dagger]$ for the three-qubit system can be derived using the subsequent equation

$$\rho_{ABC}(t) = \sum_{\mu,\nu} \rho_{\mu,\nu}(t) |\phi_\mu\rangle\langle\phi_\nu| \quad (20)$$

where $\rho_{\mu,\nu}(t)$ is written as follows

$$\rho_{\mu,\nu}(t) = \rho_{\mu,\nu}(0) F_{\mu,\nu}(t) \quad (21)$$

in this mathematical relation, $F_{\mu,\nu}(t)$ is defined as follows

$$F_{\mu,\nu}(t) = \prod_{k>0} \frac{e^{it(\xi_{k,\lambda_\mu} - \xi_{k,\lambda_\nu})}}{Z_k} \left(\mathcal{A}_k^{\lambda_\mu, \lambda_\nu} + 2e^{-\beta\xi_{k,\eta} + it(\xi_{k,\lambda_\nu} - \xi_{k,\lambda_\mu})} + e^{-2\beta\xi_{k,\eta}} \mathcal{B}_k^{\lambda_\mu, \lambda_\nu} \right) \quad (22)$$

where $\mathcal{A}_k^{\lambda_\mu, \lambda_\nu}$ and $\mathcal{B}_k^{\lambda_\mu, \lambda_\nu}$ are defined as follows

$$\begin{aligned} \mathcal{A}_k^{\lambda_\mu, \lambda_\nu} &= \left(1 - e^{2it\xi_{k,\lambda_\mu}}\right) \left(1 - e^{-2it\xi_{k,\lambda_\nu}}\right) \sin\left(\frac{1}{2}(\theta_{k,\lambda_\mu} - \theta_{k,\eta})\right) \sin\left(\frac{1}{2}(\theta_{k,\lambda_\nu} - \theta_{k,\eta})\right) \\ &\cos\left(\frac{1}{2}(\theta_{k,\lambda_\mu} - \theta_{k,\lambda_\nu})\right) - \left(\left(1 - e^{2it\xi_{k,\lambda_\mu}}\right) \sin^2\left(\frac{1}{2}(\theta_{k,\lambda_\mu} - \theta_{k,\eta})\right)\right) \\ &- \left(1 - e^{-2it\xi_{k,\lambda_\nu}}\right) \sin^2\left(\frac{1}{2}(\theta_{k,\lambda_\nu} - \theta_{k,\eta})\right) + 1 \end{aligned} \quad (23)$$

$$\begin{aligned} \mathcal{B}_k^{\lambda_\mu, \lambda_\nu} &= \left(1 - e^{2it\xi_{k,\lambda_\mu}}\right) \left(1 - e^{-2it\xi_{k,\lambda_\nu}}\right) \cos\left(\frac{1}{2}(\theta_{k,\lambda_\mu} - \theta_{k,\eta})\right) \cos\left(\frac{1}{2}(\theta_{k,\lambda_\nu} - \theta_{k,\eta})\right) \\ &\cos\left(\frac{1}{2}(\theta_{k,\lambda_\mu} - \theta_{k,\lambda_\nu})\right) - \left(\left(1 - e^{2it\xi_{k,\lambda_\mu}}\right) \cos^2\left(\frac{1}{2}(\theta_{k,\lambda_\mu} - \theta_{k,\eta})\right)\right) \\ &- \left(1 - e^{-2it\xi_{k,\lambda_\nu}}\right) \cos^2\left(\frac{1}{2}(\theta_{k,\lambda_\nu} - \theta_{k,\eta})\right) + 1 \end{aligned} \quad (24)$$

With these interpretations, we have acquired the reduced density matrix $\rho_{ABC}(t)$, that can be utilized to examine the entanglement dynamics of the target quantum state for the three-qubit system.

We employ the negativity measure to compute entanglement. For a quantum state with density matrix ρ , negativity is defined as [27]

$$N(\rho) = \frac{\|\rho^{Tj}\| - 1}{2} \quad (25)$$

In this context, ρ^{Tj} represents the partial transpose of the density matrix ρ with respect to the j component. In this study, the density matrix is denoted as $\rho_{ABC}(t)$ and j can refer to the A , B , or C subsystems. Hence, the negativity of the state mentioned is defined as

$$N_{A-BC}(\rho(t)) = \frac{\|\rho(t)^{TA}\| - 1}{2} \quad (26)$$

or

$$N_{B-CA}(\rho(t)) = \frac{\|\rho(t)^{TB}\| - 1}{2} \quad (27)$$

or

$$N_{C-AB}(\rho(t)) = \frac{\|\rho(t)^{TC}\| - 1}{2} \quad (28)$$

3 The W_ζ state serves as the initial state for the three-qubit system

In this section, we define the state W_ζ as the initial state of the system as follows:

$$|W_\zeta\rangle = \frac{1}{\sqrt{2\zeta+2}} (|100\rangle + e^{i\phi}\sqrt{\zeta}|010\rangle + e^{i\delta}\sqrt{\zeta+1}|001\rangle) \quad (29)$$

The initial density matrix of the system corresponding to this state is defined as follows:

$$[\rho_s(0)]_{W_\zeta} = \begin{pmatrix} 0 & 0 & 0 & 0 & 0 & 0 & 0 & 0 \\ 0 & \frac{1}{2} & \frac{\zeta e^{i(\delta-\phi)}}{2\sqrt{\zeta(\zeta+1)}} & 0 & \frac{e^{i\delta}}{2\sqrt{\zeta+1}} & 0 & 0 & 0 \\ 0 & \frac{\zeta e^{-i(\delta-\phi)}}{2\sqrt{\zeta(\zeta+1)}} & \frac{\zeta}{2\zeta+2} & 0 & \frac{\sqrt{\zeta} e^{i\phi}}{2\zeta+2} & 0 & 0 & 0 \\ 0 & 0 & 0 & 0 & 0 & 0 & 0 & 0 \\ 0 & \frac{e^{-i\delta}}{2\sqrt{\zeta+1}} & \frac{\sqrt{\zeta} e^{-i\phi}}{2\zeta+2} & 0 & \frac{1}{2\zeta+2} & 0 & 0 & 0 \\ 0 & 0 & 0 & 0 & 0 & 0 & 0 & 0 \\ 0 & 0 & 0 & 0 & 0 & 0 & 0 & 0 \\ 0 & 0 & 0 & 0 & 0 & 0 & 0 & 0 \end{pmatrix} \quad (30)$$

After some algebraic calculations, the density matrix of the system following interaction with the environment for this state can be expressed as a matrix and in relation to eight bases of the corresponding three qubits as shown:

$$[\rho_s(t)]_{W_\zeta} = \begin{pmatrix} 0 & 0 & 0 & 0 & 0 & 0 & 0 & 0 \\ 0 & \frac{1}{2} & \frac{\zeta F_{2,3} e^{i(\delta-\phi)}}{2\sqrt{\zeta(\zeta+1)}} & 0 & \frac{e^{i\delta} F_{2,5}}{2\sqrt{\zeta+1}} & 0 & 0 & 0 \\ 0 & \frac{\zeta (F_{2,3})^* e^{-i(\delta-\phi)}}{2\sqrt{\zeta(\zeta+1)}} & \frac{\zeta}{2\zeta+2} & 0 & \frac{\sqrt{\zeta} e^{i\phi} F_{3,5}}{2\zeta+2} & 0 & 0 & 0 \\ 0 & 0 & 0 & 0 & 0 & 0 & 0 & 0 \\ 0 & \frac{e^{-i\delta} (F_{2,5})^*}{2\sqrt{\zeta+1}} & \frac{\sqrt{\zeta} e^{-i\phi} (F_{3,5})^*}{2\zeta+2} & 0 & \frac{1}{2\zeta+2} & 0 & 0 & 0 \\ 0 & 0 & 0 & 0 & 0 & 0 & 0 & 0 \\ 0 & 0 & 0 & 0 & 0 & 0 & 0 & 0 \\ 0 & 0 & 0 & 0 & 0 & 0 & 0 & 0 \end{pmatrix} \quad (31)$$

In this case, we initially concentrate our computations solely on subsystem A . Writing out the partial transpose for this subsystem yields:

$$[\rho_s(t)]_{W_\zeta}^{TA} = \begin{pmatrix} 0 & 0 & 0 & 0 & 0 & \frac{e^{-i\delta} F_{2,5}^*}{2\sqrt{\zeta+1}} & \frac{\sqrt{\zeta} e^{-i\phi} F_{3,5}^*}{2\zeta+2} & 0 \\ 0 & \frac{1}{2} & \frac{\zeta F_{2,3} e^{i(\delta-\phi)}}{2\sqrt{\zeta(\zeta+1)}} & 0 & 0 & 0 & 0 & 0 \\ 0 & \frac{\zeta e^{-i(\delta-\phi)} F_{2,3}^*}{2\sqrt{\zeta(\zeta+1)}} & \frac{\zeta}{2\zeta+2} & 0 & 0 & 0 & 0 & 0 \\ 0 & 0 & 0 & 0 & 0 & 0 & 0 & 0 \\ 0 & 0 & 0 & 0 & \frac{1}{2\zeta+2} & 0 & 0 & 0 \\ \frac{e^{i\delta} F_{2,5}}{2\sqrt{\zeta+1}} & 0 & 0 & 0 & 0 & 0 & 0 & 0 \\ \frac{\sqrt{\zeta} e^{i\phi} F_{3,5}}{2\zeta+2} & 0 & 0 & 0 & 0 & 0 & 0 & 0 \\ 0 & 0 & 0 & 0 & 0 & 0 & 0 & 0 \end{pmatrix} \quad (32)$$

because this matrix is Hermitian, its trace norm is equal to the sum of the absolute values of the eigenvalues of the matrix. In accordance with this, the negativity relation is written as follows:

$$\begin{aligned} N_{A-BC} &= -\frac{1}{8(\zeta+1)^{5/2}\sqrt{\zeta(\zeta+1)}} \\ &(-\zeta \left| \sqrt{\zeta(\zeta+1)}(2\zeta+1) - e^{-i(\delta+\phi)} \sqrt{e^{2i(\delta+\phi)}\zeta(\zeta+1)^2 (4\zeta(\zeta+1)|F_{2,3}|^2 + 1)} \right| \\ &- \left| \sqrt{\zeta(\zeta+1)}(2\zeta+1) - e^{-i(\delta+\phi)} \sqrt{e^{2i(\delta+\phi)}\zeta(\zeta+1)^2 (4\zeta(\zeta+1)|F_{2,3}|^2 + 1)} \right| \\ &-\zeta \left| \sqrt{\zeta(\zeta+1)}(2\zeta+1) + e^{-i(\delta+\phi)} \sqrt{e^{2i(\delta+\phi)}\zeta(\zeta+1)^2 (4\zeta(\zeta+1)|F_{2,3}|^2 + 1)} \right| \\ &- \left| \sqrt{\zeta(\zeta+1)}(2\zeta+1) + e^{-i(\delta+\phi)} \sqrt{e^{2i(\delta+\phi)}\zeta(\zeta+1)^2 (4\zeta(\zeta+1)|F_{2,3}|^2 + 1)} \right| \\ &-4\sqrt{\zeta(\zeta+1)}(\zeta+1)^{3/2} \left| \sqrt{(\zeta+1)|F_{2,5}|^2 + \zeta|F_{3,5}|^2} \right| + 4\zeta\sqrt{\zeta(\zeta+1)}(\zeta+1)^{3/2} \\ &+2\sqrt{\zeta(\zeta+1)}(\zeta+1)^{3/2}) \end{aligned} \quad (33)$$

With the same calculations as before, we derive the following relationship for the partial transpose of subsystem B in this state:

$$[\rho_s(t)]_{W_\zeta}^{TB} =$$

$$\begin{pmatrix}
0 & 0 & 0 & \frac{\zeta e^{-i(\delta-\phi)F_{2,3}^*}}{2\sqrt{\zeta(\zeta+1)}} & 0 & 0 & \frac{\sqrt{\zeta}e^{i\phi}F_{3,5}}{2\zeta+2} & 0 \\
0 & \frac{1}{2} & 0 & 0 & \frac{e^{i\delta}F_{2,5}}{2\sqrt{\zeta+1}} & 0 & 0 & 0 \\
0 & 0 & \frac{\zeta}{2\zeta+2} & 0 & 0 & 0 & 0 & 0 \\
\frac{\zeta F_{2,3}e^{i(\delta-\phi)}}{2\sqrt{\zeta(\zeta+1)}} & 0 & 0 & 0 & 0 & 0 & 0 & 0 \\
0 & \frac{e^{-i\delta}F_{2,5}^*}{2\sqrt{\zeta+1}} & 0 & 0 & \frac{1}{2\zeta+2} & 0 & 0 & 0 \\
0 & 0 & 0 & 0 & 0 & 0 & 0 & 0 \\
\frac{\sqrt{\zeta}e^{-i\phi}F_{3,5}^*}{2\zeta+2} & 0 & 0 & 0 & 0 & 0 & 0 & 0 \\
0 & 0 & 0 & 0 & 0 & 0 & 0 & 0
\end{pmatrix} \quad (34)$$

this matrix is also Hermitian and its trace norm equals the sum of the absolute values of its eigenvalues. Furthermore, following the negativity relation, we can express this as:

$$\begin{aligned}
N_{B-CA} &= -\frac{1}{8(\zeta+1)^{5/2}\sqrt{\zeta(\zeta+1)}} \\
&(-\zeta \left| \sqrt{\zeta}(\zeta+1)(\zeta+2) - e^{-i(\delta+\phi)} \sqrt{e^{2i(\delta+\phi)}\zeta(\zeta+1)^2(\zeta^2+4(\zeta+1)|F_{2,5}|^2)} \right| \\
&- \left| \sqrt{\zeta}(\zeta+1)(\zeta+2) - e^{-i(\delta+\phi)} \sqrt{e^{2i(\delta+\phi)}\zeta(\zeta+1)^2(\zeta^2+4(\zeta+1)|F_{2,5}|^2)} \right| \\
&-\zeta \left| \sqrt{\zeta}(\zeta+1)(\zeta+2) + e^{-i(\delta+\phi)} \sqrt{e^{2i(\delta+\phi)}\zeta(\zeta+1)^2(\zeta^2+4(\zeta+1)|F_{2,5}|^2)} \right| \\
&- \left| \sqrt{\zeta}(\zeta+1)(\zeta+2) + e^{-i(\delta+\phi)} \sqrt{e^{2i(\delta+\phi)}\zeta(\zeta+1)^2(\zeta^2+4(\zeta+1)|F_{2,5}|^2)} \right| \\
&-4\sqrt{\zeta}\sqrt{\zeta(\zeta+1)}(\zeta+1)^{3/2} \left| \sqrt{(\zeta+1)|F_{2,3}|^2 + |F_{3,5}|^2} \right| + 2\zeta\sqrt{\zeta(\zeta+1)}(\zeta+1)^{3/2} \\
&+4\sqrt{\zeta(\zeta+1)}(\zeta+1)^{3/2}
\end{aligned} \quad (35)$$

Finally, for the partial transpose of subsystem C , we obtain the following relationship:

$$[\rho_s(t)]_{W_\zeta}^{T_C} =
\begin{pmatrix}
0 & 0 & 0 & \frac{\zeta F_{2,3}e^{i(\delta-\phi)}}{2\sqrt{\zeta(\zeta+1)}} & 0 & \frac{e^{i\delta}F_{2,5}}{2\sqrt{\zeta+1}} & 0 & 0 \\
0 & \frac{1}{2} & 0 & 0 & 0 & 0 & 0 & 0 \\
0 & 0 & \frac{\zeta}{2\zeta+2} & 0 & \frac{\sqrt{\zeta}e^{i\phi}F_{3,5}}{2\zeta+2} & 0 & 0 & 0 \\
\frac{\zeta e^{-i(\delta-\phi)F_{2,3}^*}}{2\sqrt{\zeta(\zeta+1)}} & 0 & 0 & 0 & 0 & 0 & 0 & 0 \\
0 & 0 & \frac{\sqrt{\zeta}e^{-i\phi}F_{3,5}^*}{2\zeta+2} & 0 & \frac{1}{2\zeta+2} & 0 & 0 & 0 \\
\frac{e^{-i\delta}F_{2,5}^*}{2\sqrt{\zeta+1}} & 0 & 0 & 0 & 0 & 0 & 0 & 0 \\
0 & 0 & 0 & 0 & 0 & 0 & 0 & 0 \\
0 & 0 & 0 & 0 & 0 & 0 & 0 & 0
\end{pmatrix} \quad (36)$$

it can be shown that this matrix is also Hermitian, and its trace norm equals the sum of the absolute values of its eigenvalues. Furthermore, following the negativity relation, we can express:

$$\begin{aligned}
N_{C-AB} = & -\frac{1}{8(\zeta+1)^{3/2}\sqrt{\zeta(\zeta+1)}} \\
& \left(-\left| \sqrt{\zeta}(\zeta+1)^2 - e^{-i(\delta+\phi)} \sqrt{e^{2i(\delta+\phi)}\zeta(\zeta+1)^2 (4\zeta|F_{3,5}|^2 + (\zeta-2)\zeta+1)} \right| \right. \\
& - \left. \left| \sqrt{\zeta}(\zeta+1)^2 + e^{-i(\delta+\phi)} \sqrt{e^{2i(\delta+\phi)}\zeta(\zeta+1)^2 (4\zeta|F_{3,5}|^2 + (\zeta-2)\zeta+1)} \right| \right) \\
& - 4\zeta\sqrt{\zeta(\zeta+1)} \left| \sqrt{\zeta|F_{2,3}|^2 + |F_{2,5}|^2} \right| - 4\sqrt{\zeta(\zeta+1)} \left| \sqrt{\zeta|F_{2,3}|^2 + |F_{2,5}|^2} \right| \\
& + 2\sqrt{\zeta(\zeta+1)}(\zeta+1)^{3/2}
\end{aligned} \tag{37}$$

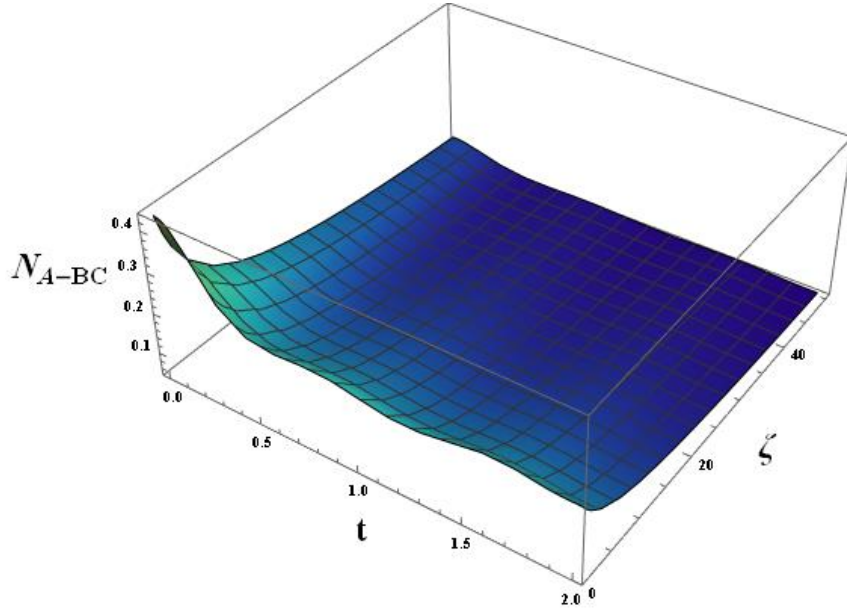


Figure 1: The 3D diagram of N_{A-BC} for state W_ζ , with respect to ζ and t for specific values of $\delta = \pi/2$, $\phi = \pi/2$, $\eta = 1$, $T = 0.5$, $\gamma = 1$, $\alpha = 1$, $g_A = 0.1$, $g_B = 0.2$, $g_C = 0.3$, and $\mathcal{N} = 51$.

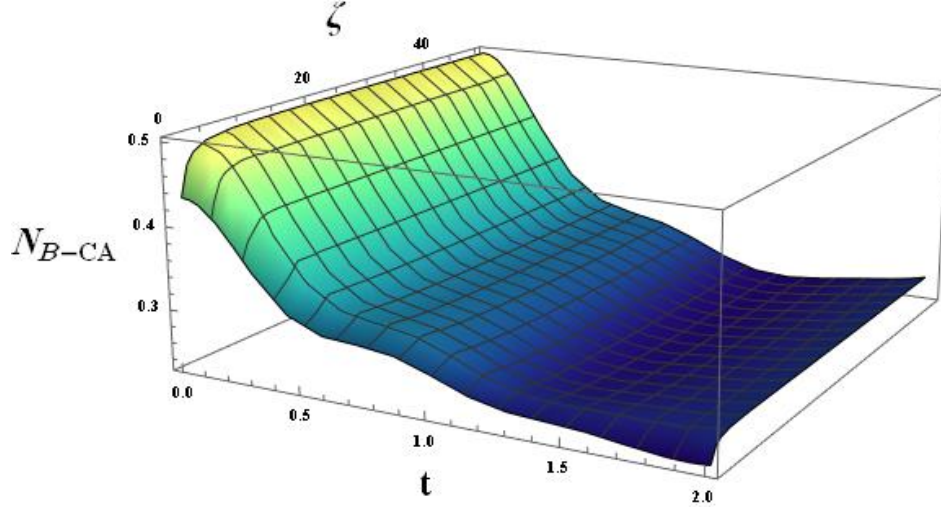


Figure 2: The 3D plot of N_{B-CA} for state W_ζ , with respect to ζ and t for specific values of $\delta = \pi/2$, $\phi = \pi/2$, $\eta = 1$, $T = 0.5$, $\gamma = 1$, $\alpha = 1$, $g_A = 0.1$, $g_B = 0.2$, $g_C = 0.3$, and $\mathcal{N} = 51$.

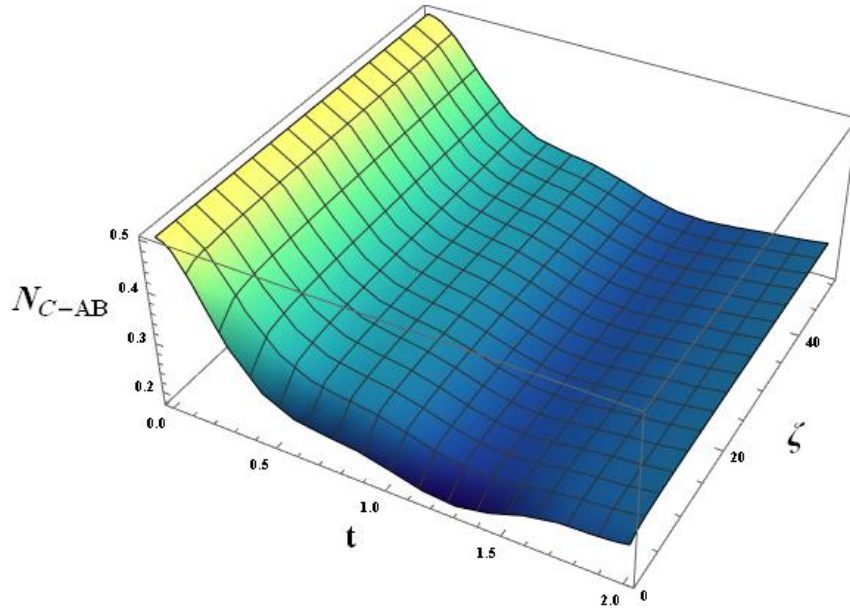


Figure 3: The 3D diagram of N_{C-AB} for the W_ζ state, with respect to ζ and t for specific values of $\delta = \pi/2$, $\phi = \pi/2$, $\eta = 1$, $T = 0.5$, $\gamma = 1$, $\alpha = 1$, $g_A = 0.1$, $g_B = 0.2$, $g_C = 0.3$, and $\mathcal{N} = 51$.

In this particular part of our study, we would like to show case and highlight the detailed computational findings and outcomes pertaining to the W_ζ state being employed as the initial condition for the triple-qubit system analysis. As previously mentioned, we have utilized the negativity criterion to analyze the dynamics of quantum entanglement.

Figure 1 shows the three-dimensional diagram of N_{A-BC} for state W_ζ , with respect to ζ and t . This figure illustrates the trend of N_{A-BC} approaching zero with some fluctuation as time progresses. As ζ increases, N_{A-BC} decreases. Initially, the decrease in N_{A-BC} is less pronounced due to increasing ζ . This instance shows the quickest decline in negativity as time and ζ increase and we see the death of entanglement from $t = 0.3$ onwards.

Figure 2 depicts the three-dimensional diagram of N_{B-CA} for state W_ζ , with respect to ζ and t . This figure demonstrates the decrease in N_{B-CA} over time. As ζ varies from 0 to 5, N_{B-CA} increases from 0 to 0.15. The negativity changes in this scenario exhibit sluggish progression with rising ζ values, however, with the passage of time, starting from $t = 1.3$, entanglement swiftly diminishes.

Figure 3 shows the three-dimensional diagram of N_{C-AB} for the W_ζ state, with respect to ζ and t . This figure shows that the fluctuation of N_{C-AB} ranges from 0 to 1.25 over time, reaching 0 at $t = 1.25$. Subsequently, N_{C-AB} rises to 0.22 between $t = 1.25$ and $t = 2$. With increasing ζ , N_{C-AB} escalates gradually from 0 to 5, hovering between 0 and 0.25, and maintaining near-constant values between 5 and 50. As depicted in Figure 2, the alterations in negativity for this scenario also exhibit a gradual pace with increasing ζ values. However, as time progresses, starting from $t = 1.3$ onwards, entanglement experiences a rapid decline.

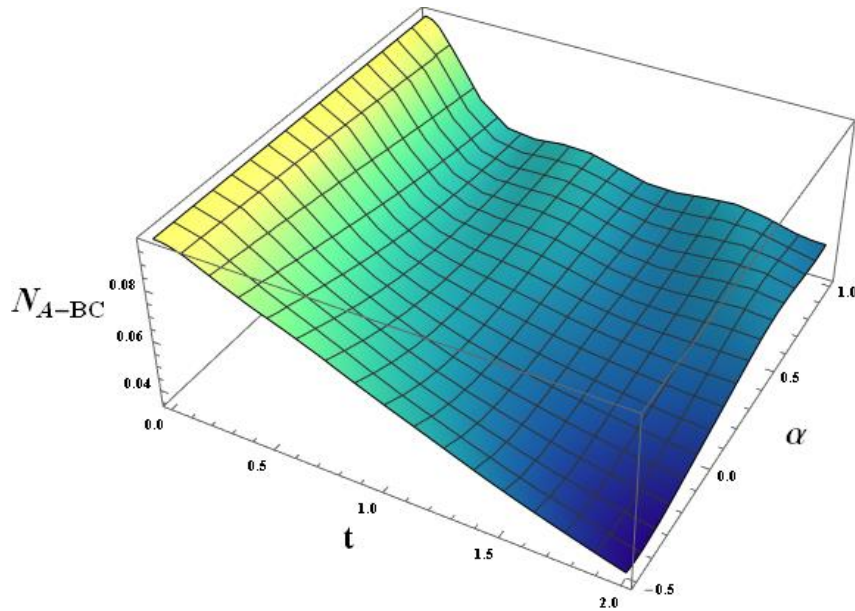


Figure 4: The 3D diagram of N_{A-BC} for W_ζ state, in relation to α and t for specific values of $\delta = \pi/2$, $\phi = \pi/2$, $\eta = 1$, $T = 0.5$, $\gamma = 1$, $\zeta = 50$, $g_A = 0.1$, $g_B = 0.2$, $g_C = 0.3$, and $\mathcal{N} = 51$.

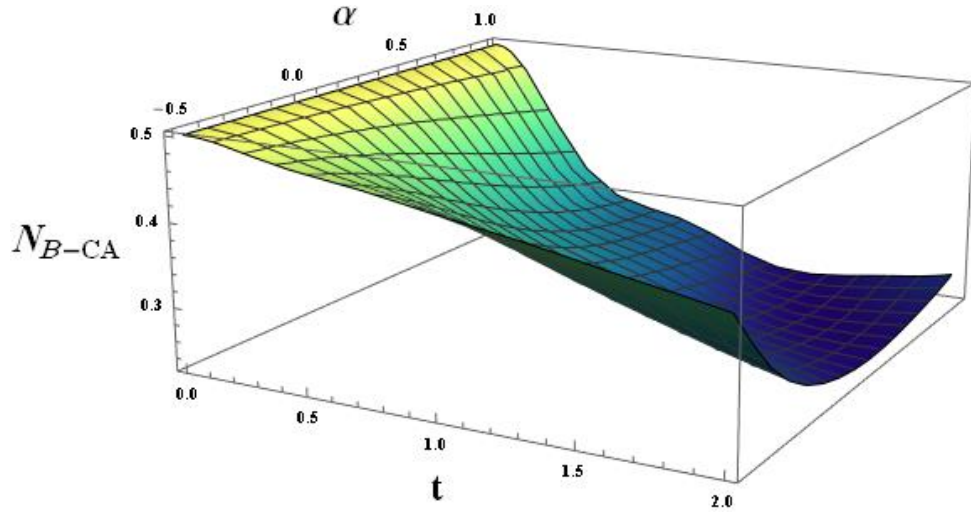


Figure 5: The 3D diagram of N_{B-CA} for state W_ζ , in relation to α and t for specific values of $\delta = \pi/2$, $\phi = \pi/2$, $\eta = 1$, $T = 0.5$, $\gamma = 1$, $\zeta = 50$, $g_A = 0.1$, $g_B = 0.2$, $g_C = 0.3$, and $\mathcal{N} = 51$.

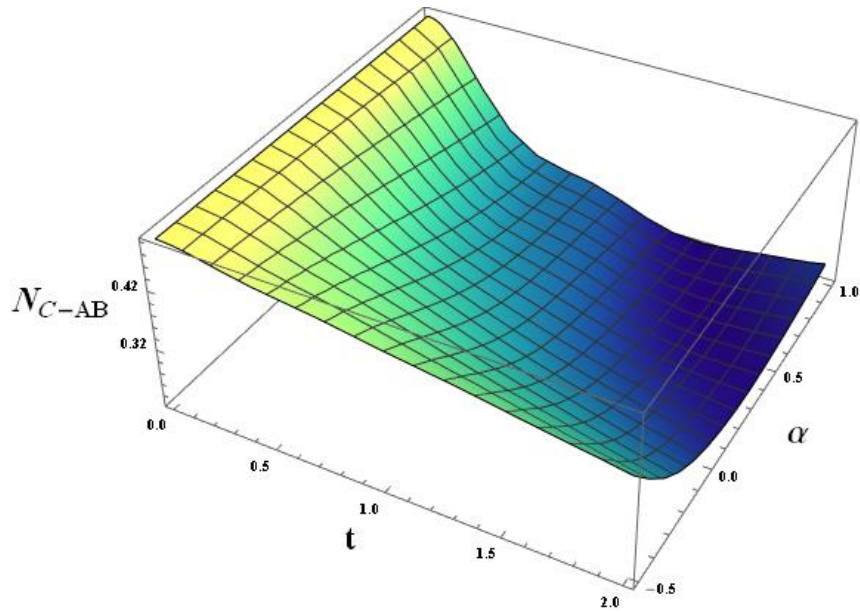


Figure 6: The 3D diagram of N_{C-AB} for state W_ζ , in relation to α and t for specific values of $\delta = \pi/2$, $\phi = \pi/2$, $\eta = 1$, $T = 0.5$, $\gamma = 1$, $\zeta = 50$, $g_A = 0.1$, $g_B = 0.2$, $g_C = 0.3$, and $\mathcal{N} = 51$.

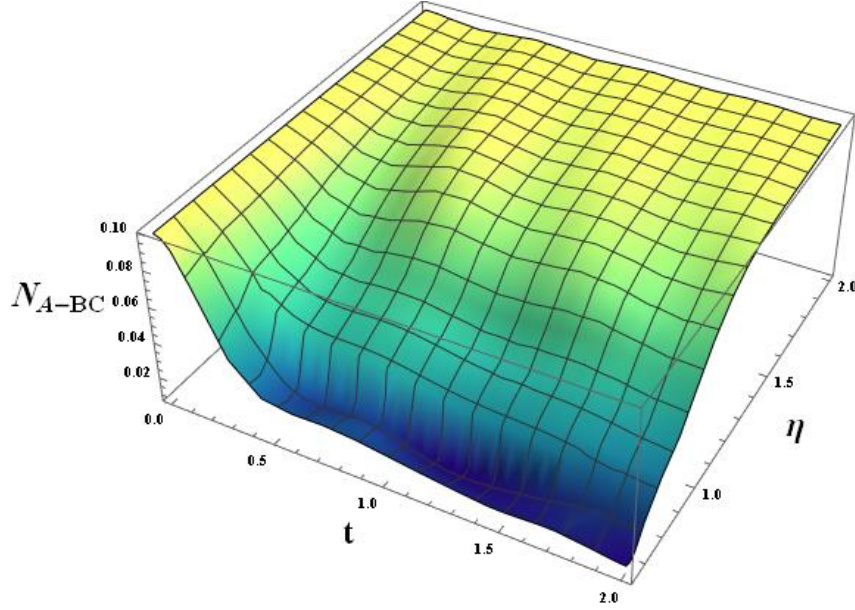


Figure 7: The 3D diagram of N_{A-BC} for state W_ζ , in relation to η and t for specific values of $\delta = \pi/2$, $\phi = \pi/2$, $\alpha = 1$, $T = 0.5$, $\gamma = 1$, $\zeta = 50$, $g_A = 0.1$, $g_B = 0.2$, $g_C = 0.3$, and $\mathcal{N} = 51$.

Figure 4 shows the three-dimensional diagram of N_{A-BC} for W_ζ state, in relation to α and t . This figure depicts the decline of N_{A-BC} with time. Decreases in α accelerate N_{A-BC} reduction over time. Conversely, as α rises, the rate of N_{A-BC} decline reduces. Transitioning from -0.5 to 1, N_{A-BC} ascends from 0 to 0.05. For $\alpha > 0$, N_{A-BC} exhibits minor fluctuations over time. In this scenario, with $\alpha = 0$, entanglement diminishes linearly as time progresses. As α increases, the rate of entanglement reduction slows down over time.

Figure 5 depicts the three-dimensional diagram of N_{B-CA} for state W_ζ , in relation to α and t . This figure shows the reduction of N_{B-CA} unfolds over time. Sluggish changes occur with lower α values, while increments in α correlate with decreases in N_{B-CA} until it reaches a minimum of 0.22 at $\alpha = 0.3$. Subsequently, an upward trend in N_{B-CA} commences, peaking at 0.26 for $\alpha = 1$. Here as well, at $\alpha = 0$, entanglement decreases linearly over time, albeit with a slightly gentler slope compared to the scenario depicted in Figure 4. As α increases, the process of entanglement reduction speeds up over time.

Figure 6 shows the three-dimensional diagram of N_{C-AB} for state W_ζ , in relation to α and t . This figure shows the declining trend of N_{C-AB} over time. Similar to N_{B-CA} , N_{C-AB} varies inversely with α , reaching a minimum of 0.24 at $\alpha = 0.35$, then ascending to 0.28 at $\alpha = 1$. In this instance, the entanglement at $\alpha = 0$ diminishes gradually over time. As α increases, the speed of entanglement reduction also increases.

Figure 7 depicts the three-dimensional diagram of N_{A-BC} for state W_ζ , in relation to η and t .

This figure shows that N_{A-BC} decreases within the time interval between $\eta = 0.65$ and $t = 0.5$ with slight fluctuations. The increase from $\eta = 0.65$ to 2 results in N_{A-BC} escalating from 0 to 1, more rapidly at lower times. Between $\eta = 1$ and 2, temporal fluctuations in N_{A-BC} emerge. In this scenario, the entanglement at $\eta = 0.65$ decreases quickly over time. As η increases, the entanglement also increases and reaches its maximum value of 0.1 at $\eta = 2$.

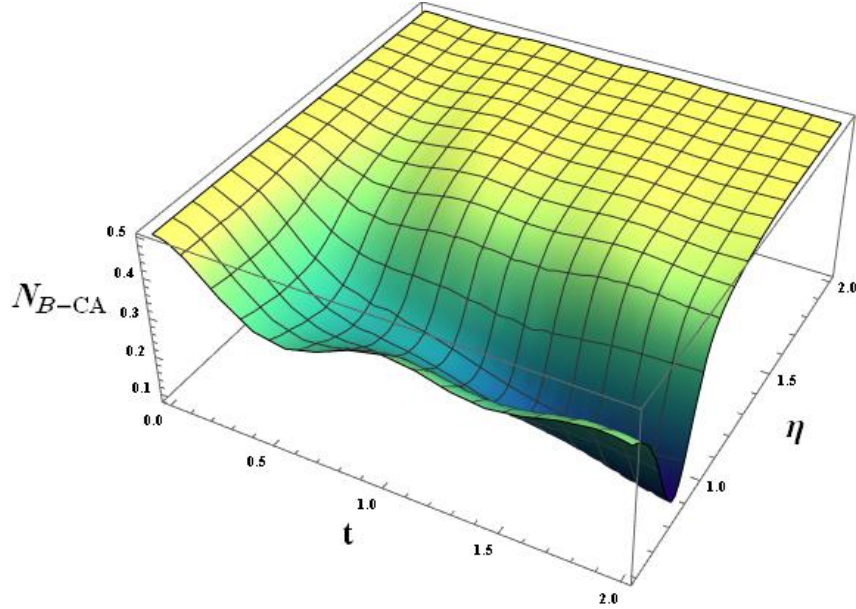


Figure 8: The 3D diagram of N_{B-CA} for state W_ζ , in relation to η and t for specific values of $\delta = \pi/2$, $\phi = \pi/2$, $\alpha = 1$, $T = 0.5$, $\gamma = 1$, $\zeta = 50$, $g_A = 0.1$, $g_B = 0.2$, $g_C = 0.3$, and $\mathcal{N} = 51$.

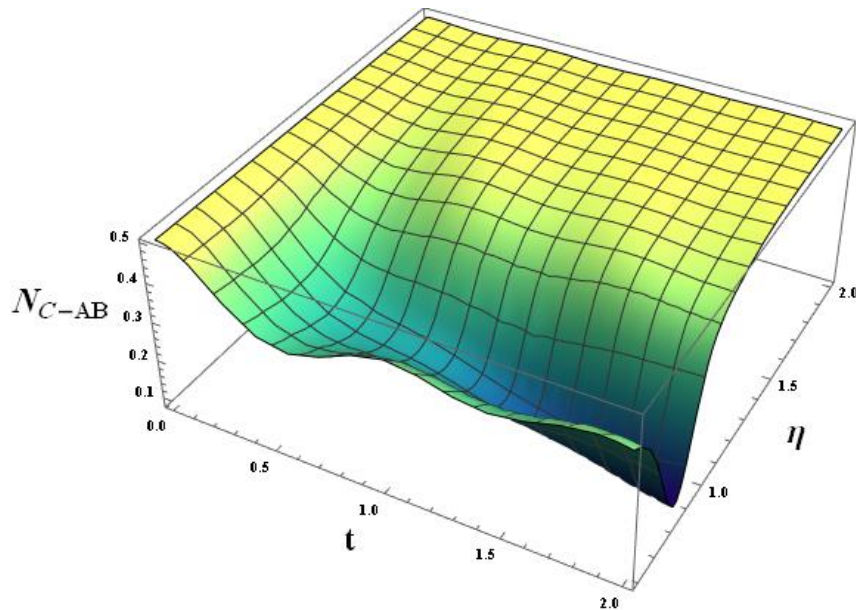


Figure 9: The 3D diagram of N_{C-AB} for the W_ζ state, with respect to η and t for specific values of $\delta = \pi/2$, $\phi = \pi/2$, $\alpha = 1$, $T = 0.5$, $\gamma = 1$, $\zeta = 50$, $g_A = 0.1$, $g_B = 0.2$, $g_C = 0.3$, and $\mathcal{N} =$

Figure 8 shows the three-dimensional diagram of N_{B-CA} for state W_ζ , in relation to η and t . This figure shows cases alternating fluctuations in N_{B-CA} at $\eta = 0.65$, with local minima at $t = 0.6$ (0.32) and $t = 1.4$ (0.37). As η climbs from 0.65 to 0.74, N_{B-CA} declines, hitting 0.1 at $\eta = 0.74$. Subsequently, a rapid ascent occurs between $\eta = 0.74$ and $\eta = 1.2$, with a more gradual increase to 0.5 from 1.2 to 2. In this scenario, for the $\eta = 0.65$, the entanglement decreases slightly over time. With the increase of η from 0.65 to 0.74, the process of entanglement reduction accelerates quickly over time. From $\eta = 0.74$ to $\eta = 1.2$, the entanglement increases swiftly. From $\eta = 1.2$ to $\eta = 2$, the entanglement increases gradually.

Figure 9 depicts the three-dimensional diagram of N_{C-AB} for the W_ζ state, with respect to η and t . This figure shows that N_{C-AB} displays similar fluctuations at $\eta = 0.65$, reaching local minima at $t = 0.6$ (0.31) and $t = 1.3$ (0.33). The negativity reduces from $\eta = 0.65$ to 0.78, hitting 0.1 at $\eta = 0.78$. Between $\eta = 0.78$ and 1.2, N_{C-AB} rises rapidly before gradually reaching 0.5 between 1.2 and 2. In this case, as in Figure 8, the discussions raised about Figure 8, for the dynamics of quantum entanglement, are still valid.

Based on the information presented, the quantum entanglement of the three-qubit system W_ζ appears to mainly decrease for the parameters ζ and α , increase for the parameter η .

Previously, the dynamics of quantum entanglement for the three-qubit states W (W_ζ state with $\zeta = 1$, $\delta = 0$ and $\phi = 0$) and GHZ has been explored by Kazemi et al. [18] and Jafarpour et al. [19], but the theoretical analysis for the W_ζ state remains unexamined.

4 Discussion and conclusions

In this particular research endeavor, we delved into the examination of the intricate quantum entanglement dynamics exhibited by the W_ζ state using the innovative Hamiltonian put forth in this scholarly work. The preliminary states taken into account are those characterized as W_ζ . Our insightful discoveries shed light on the phenomenon where entanglement experiences a decline with the amplification of the $XZY - YZX$ triplet interaction's potency, and concurrently with the mounting of the ζ parameter. Interestingly, however, there is a contrasting increase in entanglement when considering elevated values of the strength emanating from the externally applied transverse field directed towards the surrounding environment. The extensive computations undertaken in this study harmoniously align with the wealth of prior literature tackling the entanglement dynamics pertaining to a select state configuration within the enveloping W_ζ state, specifically denoted as W (a nuanced illustration of the W_ζ state with $\zeta = 1$, $\delta = 0$, and $\phi = 0$).

References

- [1] Bennett, C.H.: *Quantum Cryptography Using Any Two Nonorthogonal States*. Phys. Rev. Lett. **68**, 3121 (1992)
- [2] Bennett, C.H., Brassard, G., Crepeau, C., Jozsa, R., Peres, A., Wootters, W.K.: *Teleporting an unknown quantum state via dual classical and Einstein–Podolsky–Rosen channels*. Phys. Rev. Lett. **70**, 1899 (1993)
- [3] Ekert, A.K.: *Quantum cryptography based on Bell’s theorem*. Phys. Rev. Lett. **67**(6), 661–663 (1991)
- [4] Bennett, C.H., Wiesner, S.J.: *Communication via One- and Two-Particle Operators on Einstein-Podolsky-Rosen States*. Phys. Rev. Lett. **69**, 2881 (1992)
- [5] Acin, A., et al.: *Device-independent security of quantum cryptography against collective attacks*. Phys. Rev. Lett. **98**, 230501 (2007)
- [6] Grover, L.K.: *Quantum Mechanics helps in searching for a needle in a haystack*. Phys. Rev. Lett. **79**, 325 (1997)
- [7] Nielsen, M. A., Chuang, I. L. (2010). *Quantum Computation and Quantum Information: 10th Anniversary Edition*. Cambridge: Cambridge University Press. <https://doi.org/10.1017/CBO9780511976667>
- [8] Bose, S.: *Quantum communication through an unmodulated spin chain*. Phys. Rev. Lett. **91**, 207901 (2003)
- [9] Bennett, C., DiVincenzo, D. *Quantum information and computation*. Nature **404**, 247255 (2000). <https://doi.org/10.1038/35005001>
- [10] W.H. Zurek, Rev. Mod. Phys. **75**, 715 (2003). <https://doi.org/10.1103/RevModPhys.75.715>
- [11] M. Lucamarini, S. Paganelli, S. Mancini, Phys. Rev. A **69**, 062308 (2004). <https://doi.org/10.1103/PhysRevA.69.062308>
- [12] A. Hutton, S. Bose, Phys. Rev. A **69**, 042312 (2004). <https://doi.org/10.1103/PhysRevA.69.042312>
- [13] T. Yu, J.H. Eberly, Phys. Rev. Lett. **93**, 140404 (2004). <https://doi.org/10.1103/PhysRevLett.93.140404>
- [14] K. Roszak, P. Machnikowski, Phys. Rev. A **73**, 022313 (2006). <https://doi.org/10.1103/PhysRevA.73.022313>
- [15] L. Derkacz, L. Jakobczyk, Phys. Rev. A **74**, 032313 (2006). <https://doi.org/10.1103/PhysRevA.74.032313>
- [16] X.Y. Yuan, H.S. Goan, K.D. Zhu, Phys. Rev. B **75**, 045331 (2007). <https://doi.org/10.1103/PhysRevB.75.045331>
- [17] M. Hernandez, M. Orszag, Phys. Rev. A **78**, 042114 (2008). <https://doi.org/10.1103/PhysRevA.78.042114>
- [18] F. Kazemi, Hasanvand, N. Naderi; “*Correlation dynamics of a qubit system interacting with a qutrit environment embedded in a magnetic field*”; Eur. Phys. J. Plus, **136** (2021) 475-486.
- [19] M. Jafarpour, F. Kazemi Hasanvand, and D. Afshar; “*Dynamics of Entanglement and Measurement-Induced Disturbance for a Hybrid Qubit-Qutrit System Interacting with a Spin-Chain Environment: A Mean Field Approach*”; Commun. Theor. Phys. **67** (2017) 27–32.
- [20] H.T. Quan, Z. Song, X.F. Liu, P. Zanardi, C.P. Sun, Phys. Rev. Lett. **96**, 140604 (2006). <https://doi.org/10.1103/PhysRevLett.96.140604>

- [21] Z. Sun, X.G. Wang, C.P. Sun, Phys. Rev. A **75**, 062312 (2007).
<https://doi.org/10.1103/PhysRevA.75.062312>
- [22] X.S. Ma, A.M. Wang, Y. Cao, Phys. Rev. B **76**, 155327 (2007).
<https://doi.org/10.1103/PhysRevB.76.155327>
- [23] X.X. Yi, H.T. Cui, L.C. Wang, Phys. Rev. A **74**, 054102 (2006).
<https://doi.org/10.1103/PhysRevA.74.054102>
- [24] Y.C. Ou, H. Fan, J. Phys. A Math. Theor. **40**, 054102 (2007). doi
10.1088/1751-8113/40/10/014
- [25] Z.G. Yuan, P. Zhang, S.S. Li, Phys. Rev. A **75**, 012102 (2007).
<https://doi.org/10.1103/PhysRevA.75.012102>
- [26] Z.G. Yuan, P. Zhang, S.S. Li, Phys. Rev. A **76**, 042118 (2007).
<https://doi.org/10.1103/PhysRevA.76.042118>
- [27] X.S. Ma, H.S. Cong, J.Y. Zhang, A.M. Wang, Eur. Phys. J. D **48**, 285 (2008).
<https://doi.org/10.1140/epjd/e2008-00100-9>
- [28] S.L. Zhu, Phys. Rev. Lett. **96**, 077206 (2006).
<https://doi.org/10.1103/PhysRevLett.96.077206>
- [29] P. Zanardi, H.T. Quan, X.G. Wang, C.P. Sun, Phys. Rev. A **75**, 032109 (2007).
<https://doi.org/10.1103/PhysRevA.75.032109>
- [30] A.M. Tsvelik, Phys. Rev. B **42**, 779 (1990). <https://doi.org/10.1103/PhysRevB.42.779>
- [31] H. Frahm, J. Phys. A **25**, 1417 (1992). doi 10.1088/0305-4470/25/6/005
- [32] A.A. Zvyagin, J. Phys. A **34**, R21 (2001). doi 10.1088/0305-4470/34/41/201
- [33] A.A. Zvyagin, A. Klumper, Phys. Rev. B **68**, 144426 (2003).
<https://doi.org/10.1103/PhysRevB.68.144426>
- [34] P. Lou, W.C. Wu, M.C. Chang, Phys. Rev. B **70**, 064405 (2004).
<https://doi.org/10.1103/PhysRevB.70.064405>
- [35] W.W. Cheng, J.M. Liu, Phys. Rev. A **81**, 044304 (2010).
<https://doi.org/10.1103/PhysRevA.81.044304>
- [36] G. Vidal and R. F. Werner; "*Computable measure of entanglement*"; Phys. Rev. A **65** (2002)
032314. <https://doi.org/10.1103/PhysRevA.65.032314>